AD-A163 716 ELECTRON PRECIPITATION PATTERNS IN THE VICINITY OF A VLF TRANSMITTER(U) AEROSPACE CORP EL SEGUNDO CA SPACE SCIENCES LAB A L VAMPOLA 15 DEC 85 TR-0086(6940-05)-2 1/1

UNCLASSIFIED SD-TR-85-89 F04701-85-C-0086 F/G 4/1 NL

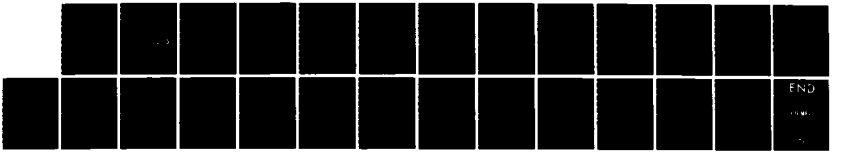

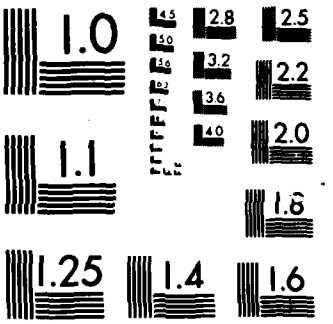

REPORT SD-TR-85-89

(12)

Electron Precipitation Patterns in the Vicinity of a VLF Transmitter

A. L. VAMPOLA
Space Sciences Laboratory
Laboratory Operations
The Aerospace Corporation
El Segundo, CA 90245

15 December 1985

APPROVED FOR PUBLIC RELEASE;
DISTRIBUTION UNLIMITED

Prepared for

SPACE DIVISION
AIR FORCE SYSTEMS COMMAND
Los Angeles Air Force Station
P.O. Box 92960, Worldway Postal Center
Los Angeles, CA 90009-2960

This report was submitted by The Aerospace Corporation, El Segundo, CA 90245, under Contract No. F04701-85-C-0086 with the Space Division, P.O. Box 92960, Worldway Postal Center, Los Angeles, CA 90009-2960. It was reviewed and approved for The Aerospace Corporation by H. R. Rugge, Director, Space Sciences Laboratory.

Capt Douglas R. Case/YCM was the project officer for the Mission-Oriented Investigation and Experimentation (MOIE) Program.

This report has been reviewed by the Public Affairs Office (PAS) and is releasable to the National Technical Information Service (NTIS). At NTIS, it will be available to the general public, including foreign nationals.

This technical report has been reviewed and is approved for publication. Publication of this report does not constitute Air Force approval of the report's findings or conclusions. It is published only for the exchange and stimulation of ideas.

Douglas R. Case

DOUGLAS R. CASE, Capt, USAF
MOIE Project Officer
SD/YCM

Joseph Hess

JOSEPH HESS, GM-15
Director, AFSTC West Coast Office
AFSTC/WCO OL-AB

UNCLASSIFIED

SECURITY CLASSIFICATION OF THIS PAGE (When Data Entered).

REPORT DOCUMENTATION PAGE	READ INSTRUCTIONS BEFORE COMPLETING FORM
1. REPORT NUMBER: SD-TR-85-89	2. GOVT ACCESSION NO.: AD-A163716
3. RECIPIENT'S CATALOG NUMBER	
4. TITLE (and Subtitle): ELECTRON PRECIPITATION PATTERNS IN THE VICINITY OF A VLF TRANSMITTER	5. TYPE OF REPORT & PERIOD COVERED
6. PERFORMING ORG. REPORT NUMBER: TR-0086(6940-05)-2	
7. AUTHOR(s): Alfred L. Vampola	8. CONTRACT OR GRANT NUMBER(s): F04701-85-C-0086
9. PERFORMING ORGANIZATION NAME AND ADDRESS: The Aerospace Corporation, El Segundo, Calif. 90245	10. PROGRAM ELEMENT, PROJECT, TASK AREA & WORK UNIT NUMBERS
11. CONTROLLING OFFICE NAME AND ADDRESS: Space Division, Los Angeles Air Force Station, Los Angeles, Calif. 90009-2960	12. REPORT DATE: 15 December 1985
	13. NUMBER OF PAGES: 21
14. MONITORING AGENCY NAME & ADDRESS(if different from Controlling Office)	15. SECURITY CLASS. (of this report): Unclassified
	15a. DECLASSIFICATION/DOWNGRADING SCHEDULE

16. DISTRIBUTION STATEMENT (of this Report)

Approved for public release; distribution unlimited.

17. DISTRIBUTION STATEMENT (of the abstract entered in Block 20, if different from Report)

18. SUPPLEMENTARY NOTES

19. KEY WORDS (Continue on reverse side if necessary and identify by block number)

Electron Precipitation
Magnetospheric Electrons
VLF Precipitation
Wave-Particle Interactions

20. ABSTRACT (Continue on reverse side if necessary and identify by block number)

Using high resolution pitch angle measurements made by a magnetic focusing electron spectrometer on the S3-3 satellite, angular distributions of 235 keV electrons precipitated by a ground-based VLF transmitter are compared with the pitch angle distributions that would be produced by various patterns of longitudinal interaction regions. The observed electrons are in the drift loss cone, necessitating the use of a trace-back-to-longitude-of-origin technique coupled with a two-dimensional convolution program

DD FORM 1473 (FACSIMILE)

UNCLASSIFIED

SECURITY CLASSIFICATION OF THIS PAGE (When Data Entered)

19. KEY WORDS (Continued)

20. ABSTRACT (Continued)

describing the response of the electron spectrometer. The data are well-fit with both theoretical calculations of ionospheric field intensity patterns above a transmitter and with a similar pattern of received field intensities measured along a traverse in the conjugate region. The agreement between the data and field patterns implies a linear or quasi-linear wave-particle interaction. The energy-frequency relationship between the electrons and the waves implies an interaction region low on the magnetic field line, perhaps near or at the unperturbed mirror point.

CONTENTS

FIGURES

INTRODUCTION

The precipitation of magnetospheric electrons by man-made waves has been discussed in the literature for a number of years. Helliwell et al.(1975) used whistler observations and band structure in chorus to demonstrate preferred magnetospheric wave frequencies which were related to power line harmonics. Bullough et al.(1976) used satellite observations of VLF wave intensities from ground stations to infer amplification of the waves, implicating electrons as the energy source. Vampola (1977) presented observations of precipitating electrons in the slot region of the magnetosphere which were grossly correlated in longitude with the location of powerful ground-based VLF transmitters. Vampola and Kuck (1978) used observations of inner zone electrons in the drift loss cone with a trace-back technique to locate the actual transmitters which were causing the precipitation. That particular paper was the first actual correlation of individual precipitation events with a single transmitter. Koons et al.(1981) used structures in the inner zone drift loss cone electron distributions and synoptic VLF data to correlate electron precipitation events with specific transmissions from the VLF transmitters UMS and NWC. Imhof et al.(1983) utilized satellite observations of precipitating electrons in the slot, obtained in conjunction with special transmitting patterns from a ground-based VLF transmitter, to obtain a one-to-one correlation between VLF transmissions and electrons in the local bounce loss cone.

While it is now generally acknowledged that man-made waves are instrumental in precipitating electrons and the mode of interaction is accepted to be a resonance between whistler-mode waves and the electron gyrofrequency (both appropriately doppler-shifted to the same frame), the precise details are still under investigation. Koons et al.(1981) utilized wave-tracing of non-ducted wave propagation to an interaction region near the equator. Vampola (1977) hypothesized wave-particle interactions much lower on the field line. Helliwell et al.(1975) utilized interactions in the equatorial region, but with ducted waves. Koons et al.(1981) calculated that a field intensity of 3 pT was sufficient to produce the scattering they observed, while a calculation of electron interaction with coherent waves reported by Inan et al.(1982) indicated that detectable electron scattering should be accomplished with as little as 1 pT.

They assumed ducting. Inan et al.(1977) reported in-situ measurements near the equator of 0.1 to 0.3 pT levels from the Siple transmitter before magnetospheric amplification. They also reported observation of an amplified wave prior to its first passage through the equatorial region, indicating that wave-particle interactions could occur well away from the equator.

Because the ionosphere is a magnetized plasma, its properties are anisotropic for radio waves reflecting off of it or propagating through it. Furthermore, it is generally highly attenuating. As a result, realistic calculations of wave propagation have not been made in analytic form. Instead, ray-tracing techniques are usually used. The advantage of ray tracing is that one can describe the propagation medium in either continuous or discrete form and make relatively good predictions of the resultant wave propagation vector and amplitude without resorting to ducts. Unfortunately, ray-tracing techniques predict passage through the ionosphere and into the magnetospheric interaction region at low latitudes even from midlatitude sources. Yet, conjugate studies show wave propagation between conjugate points. Ducting is usually given as the explanation. Direct propagation requires that an otherwise reflecting ionospheric cavity be sufficiently transparent to waves for sufficient energy to leak through to the duct.

The question of ground-based VLF transmitter wave propagation through the ionosphere into the magnetosphere can be addressed using wave-particle interaction data. Luette et al.(1977) examined the longitudinal variation in the occurrence of chorus activity on the basis that chorus was related to wave-particle interactions in which the waves were power-line harmonics. The longitudinal dependence of electron precipitation related to VLF transmitters was addressed by Vampola (1977) and Vampola and Gorney (1983), but only crude correlations with the location of ground-based sources were achieved. In this study, we will examine the precipitation pattern around a single VLF transmitter during a single event to address the question of wave energy entrance to the magnetosphere.

OBSERVATIONS AND ANALYSIS

The approach used in this investigation was to use a trace-back technique (Luhmann and Vampola, 1977) in which electrons locally observed in the drift loss cone (i.e., have mirror altitudes such that they will interact with the

atmosphere prior to or at the longitude of the South Atlantic Anomaly and hence are only quasi-trapped) are pitch-angle analyzed to determine the longitude at which their present loss-cone angle corresponds to a 100 km atmospheric loss-cone angle. This identifies the longitude of origin under the assumption that sufficient scattering has occurred to produce a loss cone defined by the local field geometry. In certain regions, most notably between 30° EL and 180° EL, this technique provides very precise answers, providing the statistical accuracy of the pitch-angle data is high and the opening angle of the instrument is small.

It appears that this type of study is not likely to benefit from a superposition of a number of different events. For one thing, different resonance conditions might occur from event to event, resulting in different energy and intensity profiles for each event. Also, the same equatorial pitch-angle distribution will provide varying local pitch-angle distributions, depending on the position of the satellite on the field line. Combining data with differing intensities and varying local pitch-angle widths per unit equatorial pitch-angle width would probably degrade the final composite distributions to the point that they would be useless for this study. Since the type of investigation we are conducting here would not benefit from a superposition of a number of different events, a single event with particularly good intensity in the precipitated electron peaks was selected. The data were obtained by a magnetic focusing spectrometer on the S3-3 satellite on 15 January 1977. The spectrometer consisted of two separate analyzing chambers, one covering the energy range 12 keV to 160 keV in five differential energy channels and another covering the range 235 keV to 1600 keV in seven differential energy channels. The lower energy unit had a collimator with a $2^{\circ}x5^{\circ}$ half-angle response, the other had a $5^{\circ}x5^{\circ}$ half-angle collimeter. The direction of scan (using the spin-stabilized spacecraft as a scanning platform) was across the 2° direction. A two-dimensional deconvolution procedure used on the data has been able to recover structure in a pitch-angle distribution to the order of 0.1° for the narrow collimator and 0.5° for the other. Particle distributions were sampled each 0.9° for this event.

While the data from the lower energy range portion of the instrument could have provided a reconstructed pitch-angle distribution to a higher degree of accuracy, this particular event was characterized by about two orders of magnitude greater flux in the 235 keV channel than in any of the others. The upper and lower limits of response of that channel are 320 keV and 158 keV, respec-

tively. Virtually all of the electrons precipitated in this event were in this energy range. The data from the 235 keV channel are shown in Fig. 1. A table at the bottom of the figure lists the geographic and geomagnetic coordinates of the satellite at the time the data were obtained. Note that this is slot data and is at a considerably higher L-value than the events reported by Vampola and Kuck (1978), Koons et al.(1981), and in a similar work by Imhof et al.(1981) in which electrons in this energy range were being precipitated in the inner zone by VLF transmitters. The L-value is similar to that of the observations of Imhof et al.(1983), but the energy is higher. The vertical dashed lines in Fig. 1 delimit the data used in the present study.

The geometry of the location of the satellite relative to the atmospheric limit of stable trapping is shown in Fig. 2. The solid line in Fig. 2 corresponds to the equatorial pitch-angle, α, of a particle which mirrors at 100 km in the northern hemisphere, plotted as a function of east longitude. For this plot, "East Longitude" refers to the longitude of the northern 100 km intercept, not the equatorial value. This was done because the combination of transmitter frequency and particle energy insures that the interaction did not take place at the equator, but rather relatively low on the field line. In Fig. 2, the "X" designates the longitude of the satellite and the equatorial pitch angle of a particle mirroring at the location of the satellite. For electrons to be observed by the satellite, they would have to have an equatorial pitch angle less than 12.2° or they would mirror above the altitude of the satellite. Also, if they had an equatorial pitch angle below 10.5°, they would be in the local loss cone; they would mirror below 100 km locally. From Fig. 2, one can see that any electrons observed by the S3-3 satellite must have had their pitch angles perturbed east of 50° EL during this drift period. The lined area indicates the limit of observation for the satellite in terms of equatorial pitch angle and east longitude. (Basically, this defines the region in which the interaction which produced the precipitated electrons of Fig. 1 occurred.)

The method of determining the interaction pattern around a transmitter (and presumably the radiation intensity above the ionosphere) will be to assume that the pitch-angle distribution observed at a given point can be represented as the sum of a number of distributions in which the original distribution is isotropic outside the local atmospheric loss cone and zero inside, at the point at which the interaction took place, and that the isotropic flux is proportional to the intensity of the waves which scattered the particles. Note that since the

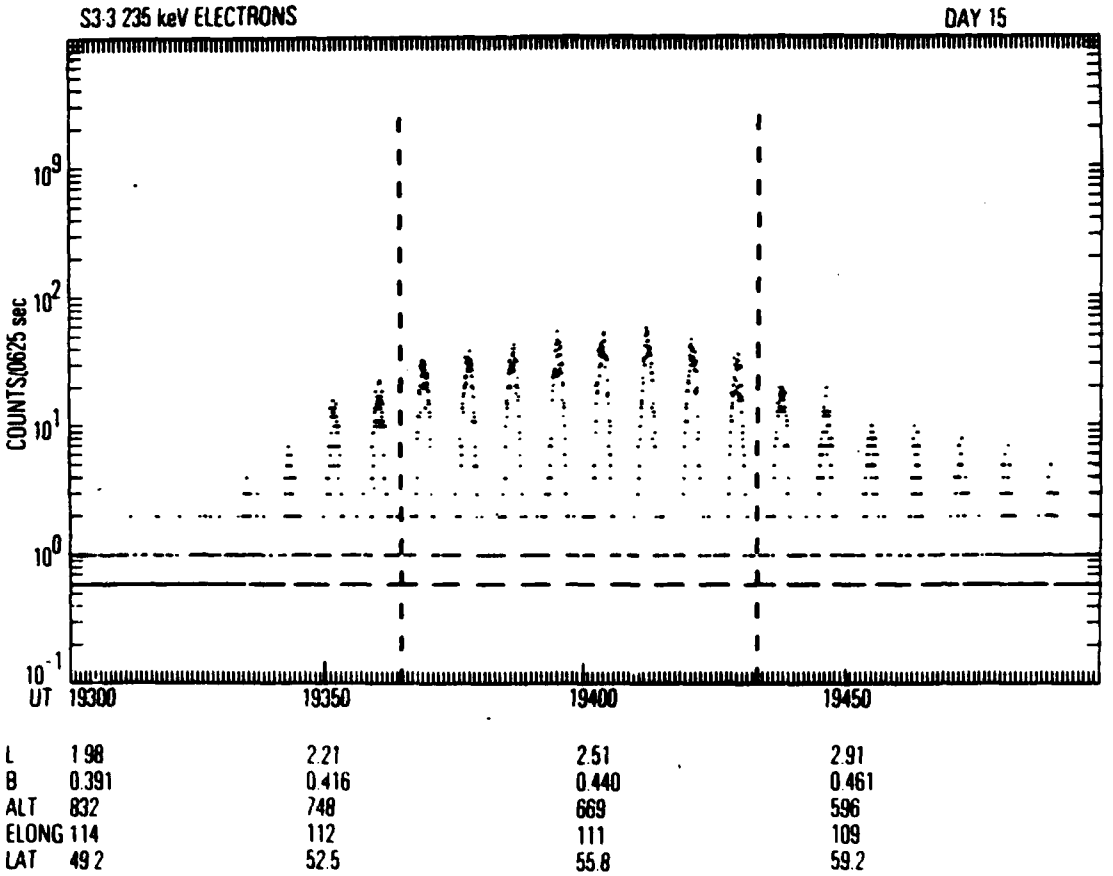

Figure 1. Electrons in the drift loss cone precipitated by a VLF transmitter on 15 January 1977. The data between the vertical dashed lines was used in this study.

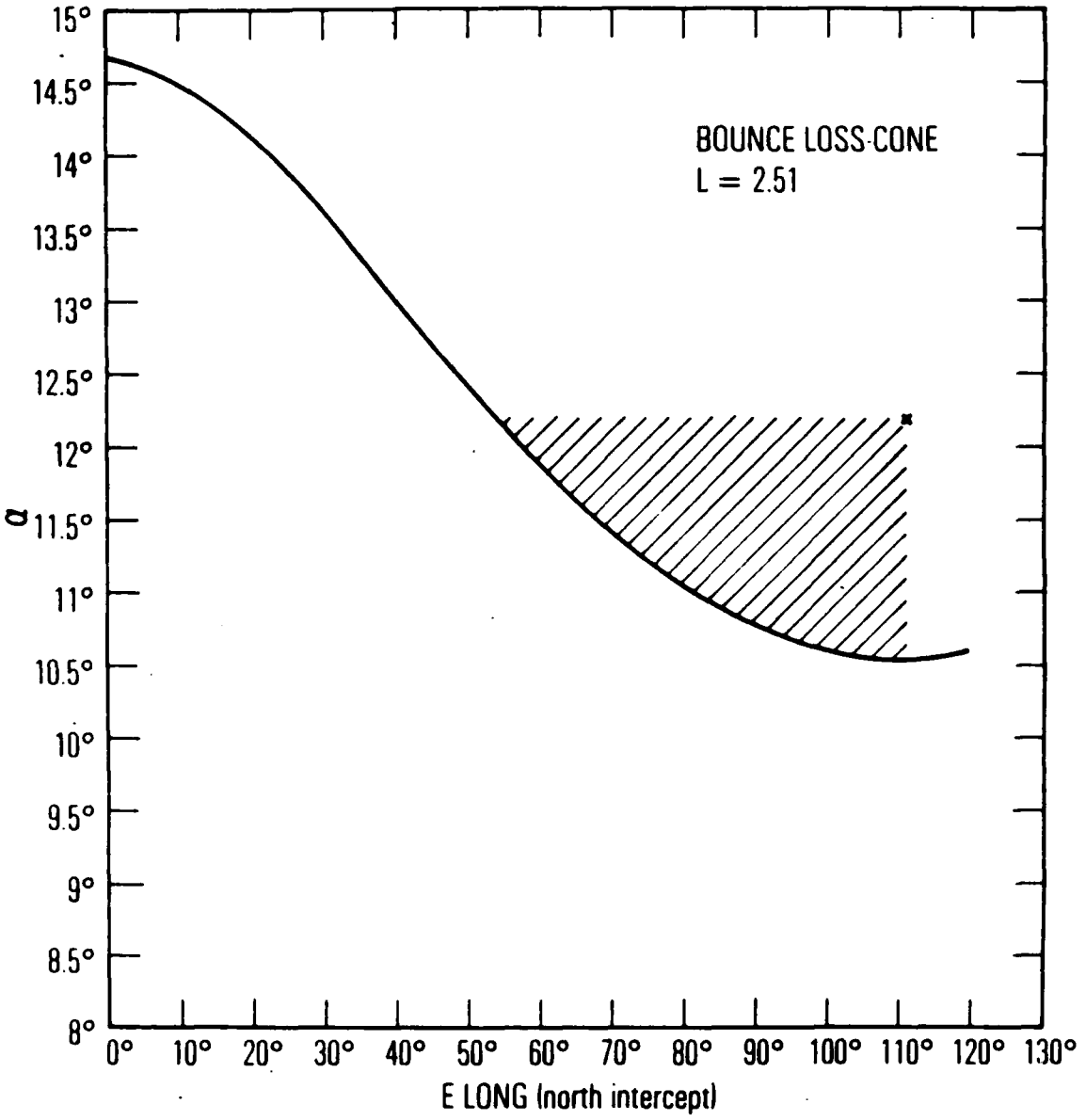

Figure 2. Plot of the equatorial pitch angle, α, of a particle mirroring at 100 km. The east longitude refers to the northern hemisphere 100 km intercept of the field line. The "x" shows the position of the S3-3 satellite for the data of Fig. 1. The lined area delineates the limits of observation of particles by the S3-3 at that time.

satellite can observe only those electrons with equatorial pitch angles below 12.2°, the original distribution need not have been completely isotropic. We require only that the distribution be isotropic between 12.2° and the angle corresponding to the local atmospheric loss cone at the location of the wave-particle interaction. The assumption of isotropy would not be valid were it not for the fact that all of the particles which are observable by the satellite at this point in space have been scattered down from farther up the field line during the immediately preceding few minutes (during the time it takes for the particles to drift from the point of scattering to the location of the satellite. Previous observations of scattering by VLF waves are consistent with isotropy in the region of scattering in and near the local bounce loss cone.

The method of reconstruction of the pattern of precipitation around a transmitter utilizes the fact that the local bounce loss cone angle is a function of east longitude and that the local pitch angle can be related to pitch angle at another location through its equatorial pitch angle. Figure 3 shows a plot of the local bounce loss cone as a function of local pitch angle and equatorial pitch angle. The dashed line represents the location of the local bounce loss cone at 110° EL. The inset presents the B and L coordinates of the satellite at that longitude. The solid curve is marked at the local bounce cone angle for various longitudes (again, northern hemisphere, 100 km altitude intercept). For the purpose of illustration, an idealized sensor with a large geometric factor and a zero opening angle would see an isotropic distribution above 77° pitch angle and zero below for an electron population which last interacted with the atmosphere at 60° EL and was unperturbed since. (In actuality, scattering in the residual atmosphere above 100 km would cause a few particles to be present with lower pitch angle, including the local bounce loss cone.)

The convolution program which was used in this investigation does not actually produce an input pitch-angle distribution from the measured data points. The program uses a knowledge of the two-dimensional response of an aperture with finite area, length, and opening angle. It includes the effects of rotational movement of the aperture during data acquisition and uses both elevation and azimuthal parameters of the aperture look direction with respect to the magnetic field line. It assumes the particle distribution is azimuthally symmetric about the field line. Given an input pitch-angle distribution function, it calculates the instrumental response to that distribution. This calculated response can be compared directly with the raw response of the instrument to a magnetospheric

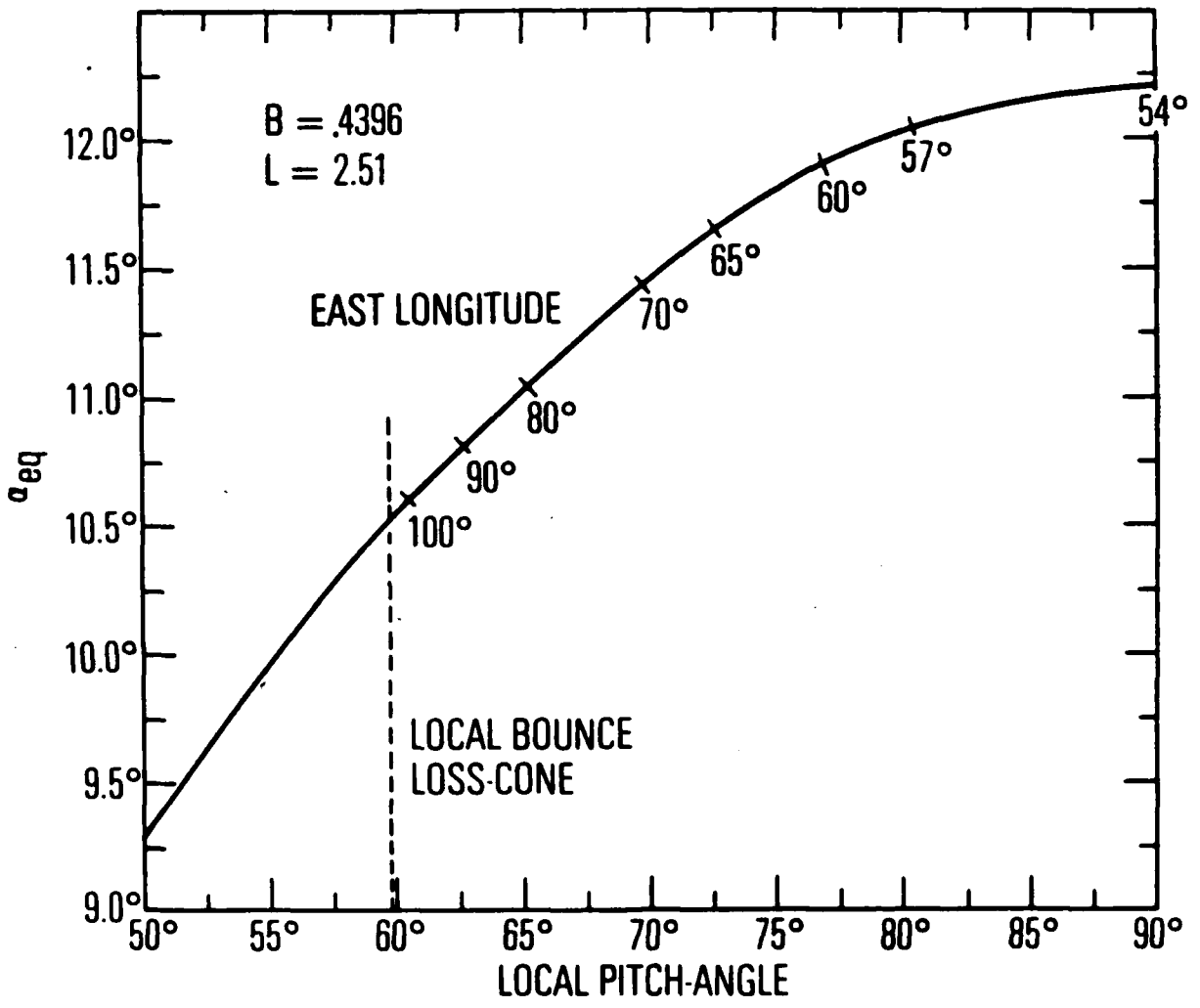

Figure 3. Plot showing the 100 km atmospheric loss cone as a function of equatorial pitch angle and local pitch angle for an observer at B = .4396 g, L = 2.51 at 110° EL in the northern hemisphere. The numbers along the curve refer to the EL at which electrons with that specific local pitch angle would have mirrored at 100 km.

distribution. In use, one makes an "educated" guess as to the original pitch-angle distribution, generates an output response with the program, compares this to the measured distribution, used the differences to assist in modifying the input distribution, and iterates. When a satisfactory match is obtained, one can be confident that the actual source distribution has been identified.

However, in our study we wish to relate the locally observed pitch-angle distribution to a longitudinal pattern of precipitation. The actual pitch-angle distribution at any location is not of interest, since it is only an intermediate step between the source function and the observed distribution. Hence, the input was actually defined in terms of a longitudinal precipitation pattern. The selection of the longitudinal precipitation patterns was somewhat arbitrary. These will be discussed later.

Since small differences near the edge of the loss cone will be needed to distinguish between several input pattern candidates, it is imperative that very good statistics are available for the data points obtained from the spectrometer. The method of improving on the statistics was to forego obtaining information about the latitudinal structure of the radiation pattern and concentrate on the longitudinal structure by averaging several peaks together to improve the statistical reliability of data points near the loss cone angle. This was done by obtaining an envelope fit to the peaks shown in Fig. 1 between the dashed lines. Note that in Fig. 1 points plotted below 1 count/.0625 sec are actually zero counts in the sample and are plotted only to show the number of samples in which no counts were observed. The parameters of the fit were used to normalize all of the other data points to the peak at about 19405 UT. Data were then averaged into 1° bins between 1° and 90° pitch angle. For this data, the spin vector of the instrument was very close to perpendicular to the local field line and data samples were obtained at all angles, including those along the field line. The normal to the aperture scanned to within less than 1° of the field line. The above binning procedure assumed that there was symmetry in the upcomming and downgoing pitch-angle distributions, which is a valid assumption provided that the distribution is in equilibrium (i.e., no significant local scattering is occurring). The large number of samples in the local loss cone which show no flux irrespective of whether it is an upcomming or downgoing sample (Fig. 1) shows the distribution is not rapidly changing. By this means, sixteen quadrants of pitch-angle measurements were averaged together, giving a typical improvement in statistical accuracy of a factor of four. The statistical

(1σ) limits for the data points plotted in the comparisons with convolution calculations in Figs. 4 and 6 are less than the size of the symbol down to about 55° pitch angle and increases up to about 1.5 times the symbol size at 50°.

RESULTS AND DISCUSSION

Figure 4 presents a comparison of the averaged electron pitch-angle distribution with four hypothetical longitudinal precipitation patterns. Figure 4a shows the distribution (dotted line) as it would be observed by the S3-3 electron spectrometer if pitch-angle scattering were occurring uniformly in longitude around the location of the transmitter with the amplitude of the scattering being independent of longitude. The longitude interval was 15°, centered on the transmitter longitude, as discussed in Koons et al. (1981). In Fig. 4a, the accumulation of flux near the local bounce loss cone produces a response that is clearly higher than the observed response. The calculated and observed responses are all normalized at 90° for Figs. 4 and 6. Figure 4b presents a comparison in which the input distribution is assumed to be approximately isotropic outside the local bounce loss cone and 1% of that level inside. The assumption of the 1% backscatter coefficient is based on experimental observations during strong diffusion precipitation events. In Fig. 4b, the predicted response near the edge of the loss cone is even greater than that of Fig. 4a and deviates strongly from the observed distribution. For the next case, Fig. 4c, a delta-function distribution over the location of the transmitter was assumed. In this case, the local atmospheric bounce loss cone at the longitude of the transmitter shapes the pitch-angle distribution and it remains unperturbed until observed by the satellite. The fit is much better in this case. In fact, it is excellent except for a critical area at the edge of the local loss cone where it is deficient in electrons. Referring back to Fig. 3, one notes that precipitation at more easterly longitudes results in flux at lower pitch angles. Hence, Fig. 4c indicates that some additional scattering must occur to the east of the transmitting site. The question is, how much additional scattering should we add and how can we justify it.

An experiment was performed (Likhter et al., 1973) in which a ship was stationed at the conjugate point of a VLF transmitter and then a second ship ran longitudinal and latitudinal traverses to obtain the ratio of received power in the transmitted signal at the two locations. For the present study, the traverse

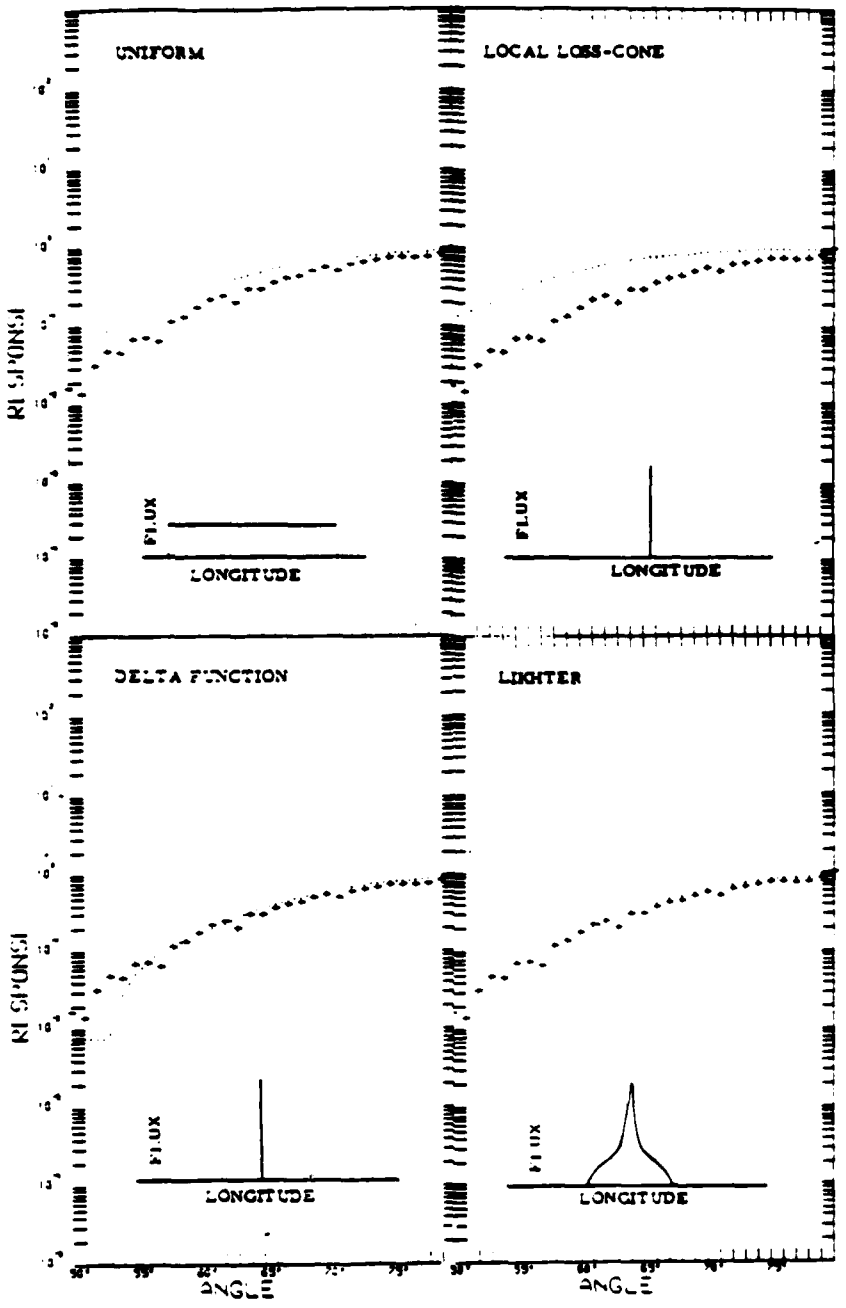

Figure 4. Comparisons between the averaged pitch-angle distribution of the electrons of Fig. 1 (symbols) and the calculated instrumental response for a precipitation pattern of the type shown in the cartoon.

data were translated into longitudinal precipitation intensity data, centered at the transmitter longitude, and used as an input source function by the convolution program. The result, Fig. 4d, is again an excellent fit and is a significant improvement over that of Fig. 4c in the critical loss cone area. Note that for both Figs. 4c and 4d the predicted flux above 80° local pitch angle is essentially isotropic, as is the actual measured pitch-angle distribution. Below 50°, both the predicted response and the measured response (within statistics) are isotropic, though at a much lower intensity. (The calculation assumes that any flux which appears within the local atmospheric loss cone is isotropized with a 1% reflection coefficient.) The small deviation between 51° and 54° local pitch angle in Fig. 4d may be due to scattering by the residual atmosphere during the drift time from the location of precipitation to the location of observation or it could be due to some other, unknown, scattering event or scattering mechanism. We do not favor scattering by the residual atmosphere as the origin since such scattering should be large-angle scattering which would essentially isotropize the scattered flux rather than causing a build-up in flux just at the edge of the loss cone. The origin of this excess is more likely due to a process which changes pitch angles slowly.

Since the Likhter et al. data extended over only a factor of ten in intensity, the possibility existed that transmitter energy at lower levels was present at greater longitudinal distance from the transmitting site. Since no experimental measurements were available to pursue this question, and since additional precipitation at greater longitudinal distances could be accommodated by the discrepancy between the observed and calculated responses of Fig. 4c, theoretical predictions of ionospheric wave intensities were used. Figure 5 presents calculations of field intensity in the ionosphere for two different waveguide models at a frequency of 15.5 kHz (which is appropriate for our study). The theoretical predictions are from Helliwell (1965) using a procedure devised by Crary (1961). Crary also calculated exit point intensities and got results similar to those of the later Likhter et al. (1973). Note that Fig. 5 differs qualitatively in profile from the Likhter et al. profile (inset, Fig. 4d). The Crary calculation predicts a null in the pattern immediately over the transmitting antenna. The null is not present in the Crary exit point profile.

Since the wave-particle interaction is presumably occurring relatively low on the field line over the transmitting site, the input profile (assuming the Crary calculation is valid) should provide a better fit than the exit profile. The final

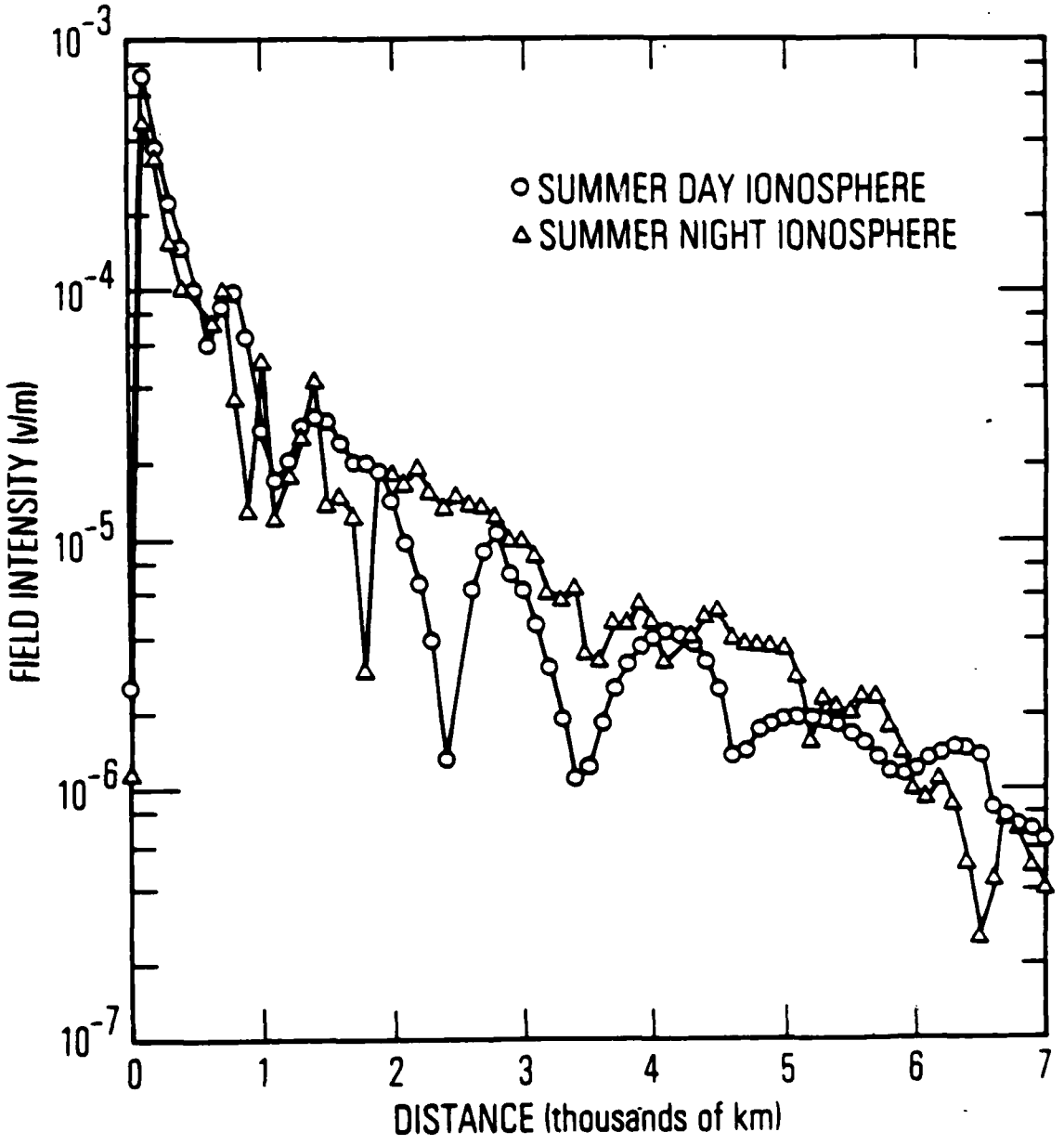

Figure 5. Calculated ionospheric field intensity for a VLF transmitter using the method of Crary (1961).

figure, Fig. 6, shows the comparison between the Crary profile (smoothed as shown in the cartoon inset of Fig. 6) and the S3-3 data. The Crary profile provides a slightly better fit to the data than the Likhter et al. profile, but the difference is small--certainly smaller than the confidence limits we can place on the individual data points obtained from the S3-3 instrumentation. When we averaged the four spin periods of data in Fig. 1, we introduced a potential obscuring factor by also averaging over latitude (the S3-3 satellite is in a polar orbit). The equatorial pitch angle of the atmospheric loss cone does not change significantly over this latitudinal variation, but the transmitter field intensity is probably azimuthally symmetric and the earth's magnetic field is slightly skewed (running slightly northwest to southeast). The azimuthal symmetry would produce a slight artificial enhancement in the averaged flux at the longitude of the transmitter and the skewing of the field would shift some of the averaged flux to slightly western longitudes (based on the fact that the flux intensities in Fig. 1 are slightly higher at higher latitude). Both of these effects are small, but because they were not eliminated from the analysis as possible obscuring factors and because the difference between the fits to the Crary and Likhter profiles is small, we cannot properly address the question of whether there is a null in the transmitter pattern immediately over the transmitting site even though the Crary pattern gives a marginally better fit. If the non-corrected effects mentioned above are responsible for the slight excess of flux in the 51° to 54° pitch-angle distribution comparisons of Figs 4d and 6, a similar analysis with an event with much better statistics in a single traverse of the 0° to 90° local pitch-angle space might provide the answer. The S3-3 data set is very large and identification of a precipitation event is a slow process. It is not known at this time whether a precipitation event meeting more stringent criteria exists in the S3-3 data set.

A most important point to make is that precipitation intensity as a function of longitude around a transmitter has been shown to be very similar (possibly identical) to the radiation pattern calculated for leakage through the ionosphere and to received signal strength measured at the conjugate point. This implies that the wave-particle interaction for these events is linear or is a quasi-linear process rather than an initiated instability, and that either the waves are ducted parallel to the field line above the ionosphere or the wave-particle interaction occurs very low on the field line. Because of the relatively low frequency of the waves compared to the energy of the particle, it is likely that the interaction

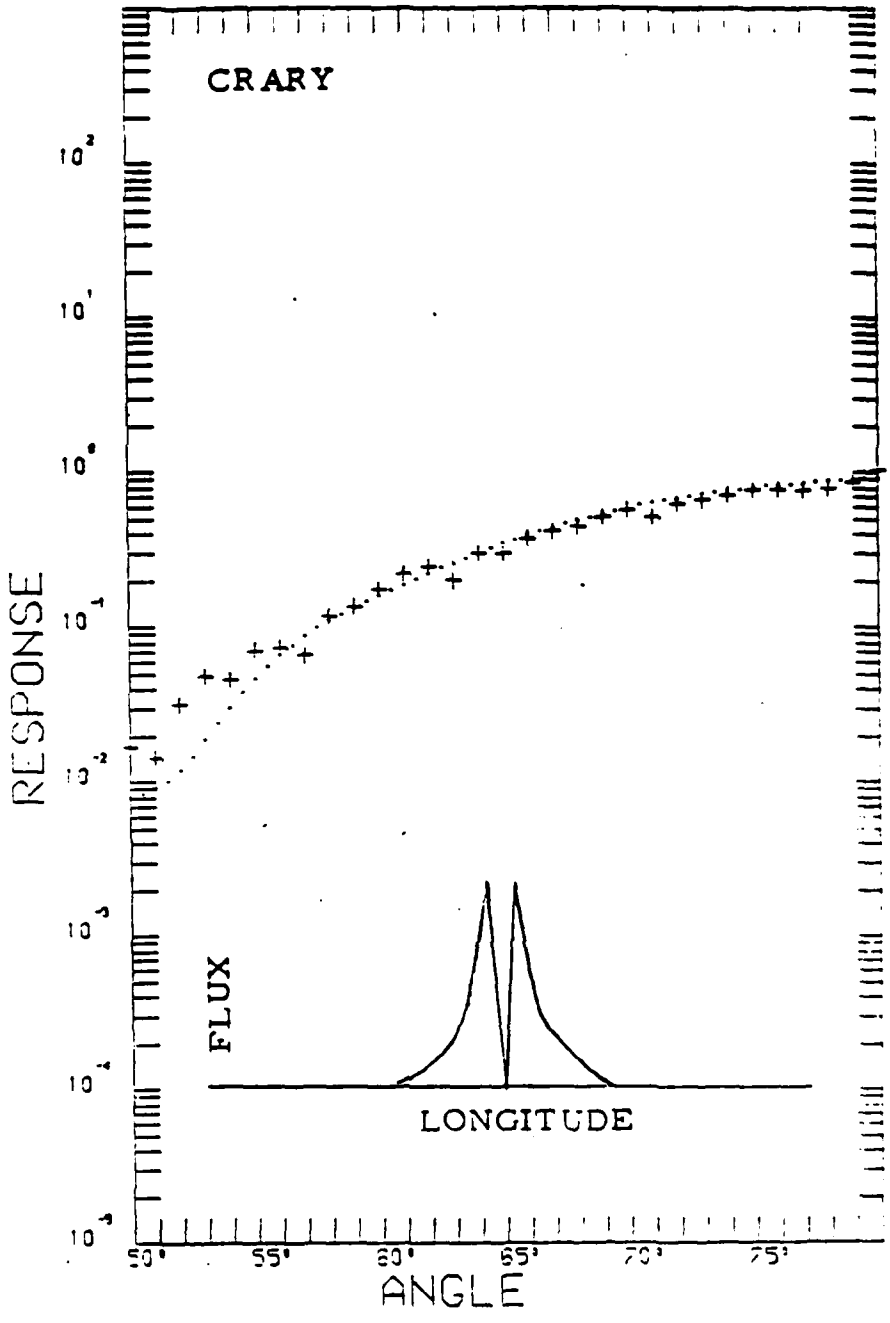

Figure 6. Plot similar to Fig. 4, but using the Crary (1961) ionospheric field intensity pattern.

is taking place relatively near to the mirror points of the particles where the longitudinal velocity of the electrons is low.

SUMMARY

An individual electron precipitation event produced by an interaction between the electrons and waves from a ground-based VLF transmitter has been studied using data from the S3-3 magnetic electron spectrometer. High resolution pitch-angle distribution data has been compared with the expected distribution from model longitudinally-dependent wave-particle interaction regions. The data are fit well with interaction regions linearly related to the field intensity predicted above a transmitter on theoretical grounds and experimentally measured at a region conjugate to a transmitter. The measured pitch-angle distributions do not resemble the distributions expected from uniform precipitation in a broad region around a transmitter. A delta-function precipitation pattern immediately over a transmitter gives a fairly good fit, but is clearly deficient in electrons which would have been precipitated both to the east and to the west of the transmitter.

The excellence of the comparison between measured pitch-angle distribution and the distribution predicted on the basis of field patterns around the transmitter indicates that the amount of precipitation is linearly related to the field intensity; therefore, the wave-particle interaction is a linear or quasi-linear process, as opposed to a process in which an instability is triggered by the wave.

Finally, the energy-frequency relationship of the particles and waves involved in the interaction indicates that the interaction region is low on the field line, where the magnetic field is large and the particle has small velocity along the field line because it is near the mirror point.

REFERENCES

Bullough, K., A. Tatnall and M. Denby, Man-made elf/vlf emissions and the radiation belts, Nature, 260, 401, 1976

Crary, J. H., The effect of earth-ionosphere waveguide on whistlers. Technical Report No. 9, Air Force Contract No. AF 18(603)-126, Radioscience Lab, Stanford Univ., Stanford, CA, 1961

Helliwell, R. A., Whistlers and Related Ionospheric Phenomena, Stanford University Press, Stanford, CA, 1965, p. 76

Helliwell, R. A., J. P. Katsufrakis, T. F. Bell, and R. Raghuram, VLF line radiation in the earth's magnetosphere and its association with power system radiation, J. Geophys. Res., 80, 4249, 1975

Imhof, W. L., R. R. Anderson, J. B. Reagan, and E. E. Gaines, The significance of vlf transmitters in the precipitation of inner belt electrons, J. Geophys. Res., 86, 11225, 1981

Imhof, W. L., J. B. Reagan, H. D. Voss, E. E. Gaines, D. W. Datlowe, J. Mobilia, R. A. Helliwell, U. S. Inan, J. Katsufrakis, and R. G. Joiner, Direct observation of radiation belt electrons precipitated by the controlled injection of VLF signals from a ground-based transmitter, Geophys. Res. Lett., 10, 361, 1983

Inan, U. S., T. F. Bell, D. L. Carpenter, and R. R. Anderson, Explorer 45 and Imp 6 observations in the magnetosphere of injected waves from the Siple Station VLF transmitter, J. Geophys. Res., 82, 1177, 1977

Inan, U. S., T. F. Bell, and H. C. Chang, Particle precipitation induced by short-duration VLF waves in the magnetosphere, J. Geophys. Res., 87, 6243, 1983

Koons, H. C., B. C. Edgar and A. L. Vampola, Precipitation of inner zone electrons by whistler mode waves from the VLF transmitters UMS and NWC, J. Geophys. Res., 86, 640, 1981

Likhter, Ya. I., O. A. Molchanov, V. M. Chmyrev, V. O. Rapoport, V. Yu. Trakhtengerts and V. A. Cherepovitsky, Modulation of spectrum and amplitude of VLF signal in the magnetosphere, Space Research XIII, Akademie-Verlag, Berlin, 1973, p. 689

Luette, J. P., C. G. Park and R. A. Helliwell, Longitudinal variations of very low frequency chorus activity in the magnetosphere; Evidence of excitation by electrical power transmission lines, Geophys. Res. Lett., 4, 275, 1977

Luhmann, J. G. and A. L. Vampola, Effects of localized sources on quiet time plasmasphere electron precipitation, J. Geophys. Res., 82, 2671, 1977

Vampola, A. L., VLF transmission-induced slot electron precipitation, Geophys. Res. Lett., 4, 569, 1977

Vampola, A. L. and G. A. Kuck, Induced precipitation of inner zone electrons 1. Observations, J. Geophys. Res., 83, 2543, 1978

Va mpola, A. L., Observations of VLF transmitter-induced depletions of inner zone electrons, Geophys. Res. Lett., 10, 619, 1983

Vampola, A. L. and D. J. Gorney, Electron energy deposition in the middle atmosphere, J. Geophys. Res., 88, 6267, 1983

LABORATORY OPERATIONS

The Aerospace Corporation functions as an "architect-engineer" for national security projects, specializing in advanced military space systems. Providing research support, the corporation's Laboratory Operations conducts experimental and theoretical investigations that focus on the application of scientific and technical advances to such systems. Vital to the success of these investigations is the technical staff's wide-ranging expertise and its ability to stay current with new developments. This expertise is enhanced by a research program aimed at dealing with the many problems associated with rapidly evolving space systems. Contributing their capabilities to the research effort are these individual laboratories:

Aerophysics Laboratory: Launch vehicle and reentry fluid mechanics, heat transfer and flight dynamics; chemical and electric propulsion, propellant chemistry, chemical dynamics, environmental chemistry, trace detection; spacecraft structural mechanics, contamination, thermal and structural control; high temperature thermomechanics, gas kinetics and radiation; cw and pulsed chemical and excimer laser development including chemical kinetics, spectroscopy, optical resonators, beam control, atmospheric propagation, laser effects and countermeasures.

Chemistry and Physics Laboratory: Atmospheric chemical reactions, atmospheric optics, light scattering, state-specific chemical reactions and radiative signatures of missile plumes, sensor out-of-field-of-view rejection, applied laser spectroscopy, laser chemistry, laser optoelectronics, solar cell physics, battery electrochemistry, space vacuum and radiation effects on materials, lubrication and surface phenomena, thermionic emission, photosensitive materials and infrared detectors, atomic frequency standards, and environmental chemistry.

Computer Science Laboratory: Program verification, program translation, performance-sensitive system design, distributed architectures for spaceborne computers, fault-tolerant computer systems, artificial intelligence, microelectronics applications, communication protocols, and computer security.

Electronics Research Laboratory: Microelectronics, solid-state device physics, compound semiconductors, radiation hardening; electro-optics, quantum electronics, solid-state lasers, optical propagation and communications; microwave semiconductor devices, microwave/millimeter wave measurements, diagnostics and radiometry, microwave/millimeter wave thermonic devices; atomic time and frequency standards; antennas, RF systems, electromagnetic propagation phenomena, space communication systems.

Materials Sciences Laboratory: Development of new materials: metals, alloys, ceramics, polymers and their composites, and new forms of carbon; nondestructive evaluation, component failure analysis and reliability; fracture mechanics and stress corrosion; analysis and evaluation of materials at cryogenic and elevated temperatures as well as in space and enemy-induced environments.

Space Sciences Laboratory: Magnetospheric, auroral and cosmic ray physics, wave-particle interactions, magnetospheric plasma waves; atmospheric and ionospheric physics, density and composition of the upper atmosphere, remote sensing using atmospheric radiation; solar physics, infrared astronomy, infrared signature analysis; effects of solar activity, magnetic storms and nuclear explosions on the earth's atmosphere, ionosphere and magnetosphere; effects of electromagnetic and particulate radiations on space systems; space instrumentation.

. . .

END

FILMED

3-86

DTIC